2

Silver Thin Film Characterization

2.1 Introduction

Thin films of Ag layered structures, typically less than a micron in thickness, are tailored to achieve desired functional properties. Typical characterization is the instrumentations that use X-ray and ion beams to probe the properties of the film. This work discusses two techniques in thin film analysis, Rutherford backscattering spectrometry (RBS) [1, 2] and X-ray diffractrometry (XRD) [3, 4] which emphasize composition and lattice measurements, respectively. Advancement in RBS and X-ray analyses are developed in response to the needs of the microelectronics and forensic disciplines.

Analysis of metallization on SiO_2 is typically done with Rutherford backscattering at 2.0 MeV energies and with semiconductor nuclear particle detectors. The resonance analysis of these species is done in the same experimental chamber as used in RBS, but the energy of the incident helium ions is increased to energies where there are resonances in the backscattering cross sections [5, 6]. These resonances increase the yield of the scattered particle by nearly two orders of magnitude and provide high sensitivity to the analysis of oxygen and carbon in silicon. The use of these high energies, 3.05 and 3.7 MeV for the helium-oxygen and helium-nitrogen resonances respectively is called resonance scattering or non-Rutherford scattering.

In a similar manner XRD is also considered as a nondestructive characterization technique. XRD is used to monitor the phases and structure present in the film. Also the lattice parameter, strain and texturing can be resolved using pole figure analysis [3, 4].

2.2 Rutherford Backscattering Spectrometry

In a typical scattering chamber, the sample is located such that the beam position does not shift across the sample as the sample is tilted with respect to the incident ion beam. The backscattering detector is mounted as close to the incident beam as possible such that the average backscattering angle, ϑ, is close to 180°, typically 170°, with a detector solid angle of 5 millisteradians (msr). The vacuum requirements in the target chamber are comparable to those in the accelerator beam lines. Enhanced vacuum levels reduce the probability that the ion beam will lose energy along its path to the sample and also minimizes deposition of contaminants and hydrocarbons on the surface during analysis.

In traditional backscattering spectrometry using helium ions, the energy resolution of the solid-state particle detector is typically >17 keV. The output signal, which is typically millivolts in pulse height is processed by silicon integrated circuit electronics and provides an energy spectrum in terms of number of particles versus energy. A multichannel analyzer records the number of backscattered particles versus a given energy in a specific channel.

2.2.1 Scattering Kinematics

During ion-beam analysis the incident particle penetrates into the target and undergoes inelastic collisions with the electrons in the samples and loses energy as it penetrates. During the penetration of the helium ions a small fraction undergo elastic collisions with the target atom, which defines the backscattering signal. Figure 2.1 shows a schematic representation of the geometry of an elastic collision between a projectile of mass M_1 and energy E_o with a target atom of mass M_2 initially at rest. After collision the incident ion is scattered back through an angle ϑ and emerges from the sample with an energy E_1. The target atom after collision has a recoil energy E_2. There is no change in target mass, because nuclear reactions are not involved and energies are non-relativistic. The ratio of the projectile energies for $M_1 < M_2$ is given by:

$$K = \frac{E_1}{E_o} = \left[\frac{(M_2^2 - M_1^2 \sin^2 \vartheta)^{\frac{1}{2}} + M_1 \cos \vartheta}{M_2 + M_1} \right]^2 \tag{2.1}$$

The energy ratio $K = E_1/E_o$, called the *kinematic factor*, shows how the energy of the backscattered particle is a function of the incident particle and target atoms masses, the scattering angle, and incident energy.

The ability to identify different mass species depends on the energy resolution of the detector which is typically 17 keV full width at half maximum (FWHM). For example, Ag has a mass $M_2 = 108$ and In has a mass $M_2 = 115$. The difference between $K_{Ag} = 0.862$ and $K_{In} = 0.870$ is 0.008. For 2.8 MeV helium ions, the difference in backscattering energy is 22 keV which is larger than the detector-system resolution, indicating that signals from Ag and In on the surface can be resolved.

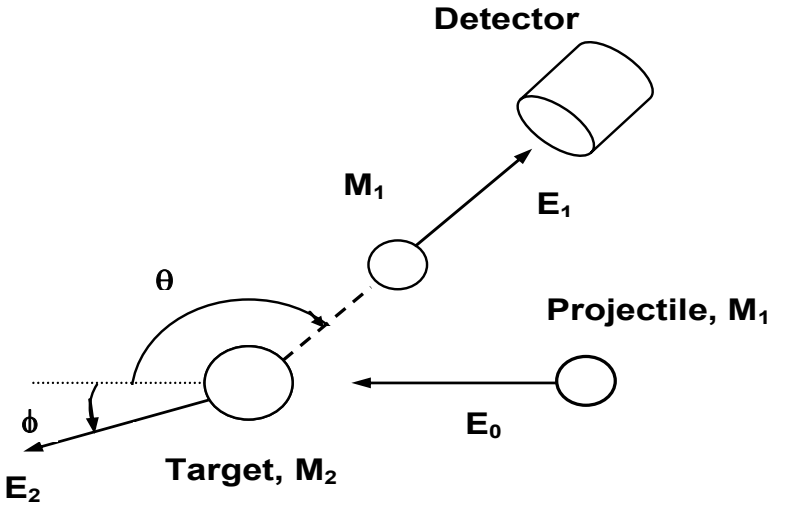

Figure 2.1. A schematic representation of an elastic collision between a particle of mass M_1 and initial energy E_0 and a target atom of mass M_2. After the collision the projectile and target atoms have energies of E_1 and E_2, respectively.

2.2.2 Scattering Cross Section

The identity of target elements is established by the energy of the scattered particles after an elastic collision. This is done by measuring the yield *Y*, the number of backscattered particles for a given value of incident particles *Q*. The detector's solid angle is given as Ω. The areal density, the number of atoms per unit area, N_S is determined from the scattering cross section σ (ϑ) by:

$$N_s = \frac{Y}{\sigma(\vartheta) Q d\Omega} \tag{2.2}$$

For a narrow beam of fast particles impinging upon a thin uniform target that is wider than the beam and at an tilt angle ϑ, the simplest approximation for the scattering cross section is given by:

$$\sigma(\vartheta) = \left(\frac{Z_1 Z_2 e^2}{4E}\right)^2 \cdot \frac{1}{\sin^4 \frac{\vartheta}{2}} \tag{2.3}$$

which is the scattering cross section originally derived by Rutherford. For 2 MeV helium ions incident on silver, Z_2 = 47 at an angle of 180º, the cross section is 2.9×10^{-24} cm^2 or 2.9 barns (where the barn = 10^{-24}cm^2). The distance of closest

approach is about 7×10^{-3} nm which is smaller than the *K*-shell radius of silver (10^{-1} nm).

2.2.3 Depth Scale

Light ions such as helium lose energy through inelastic collision with atomic electrons. In backscattering spectrometry, where the elastic collision takes place at depth *t* below the surface, one considers the energy loss along the inward path and on the outward path as shown in Figure 2.2. The energy loss on the way in is weighted by the kinematic factor and the total is given by the relationship:

$$\Delta E = \Delta t\left(K\frac{dE}{dx}\bigg|_{in} + \frac{1}{|\cos\vartheta|}\cdot\frac{dE}{dx}\bigg|_{out}\right) = \Delta t[S] \tag{2.4}$$

where d*E*/dx is the rate of energy loss with distance and [*S*] is the energy loss factor. The particle loses energy ΔE_{in} via inelastic collisions with electrons along the inward path. There is energy loss ΔE_s in the elastic scattering process at depth *t*. There is energy loss due to inelastic collisions ΔE_{out} along the outward path.

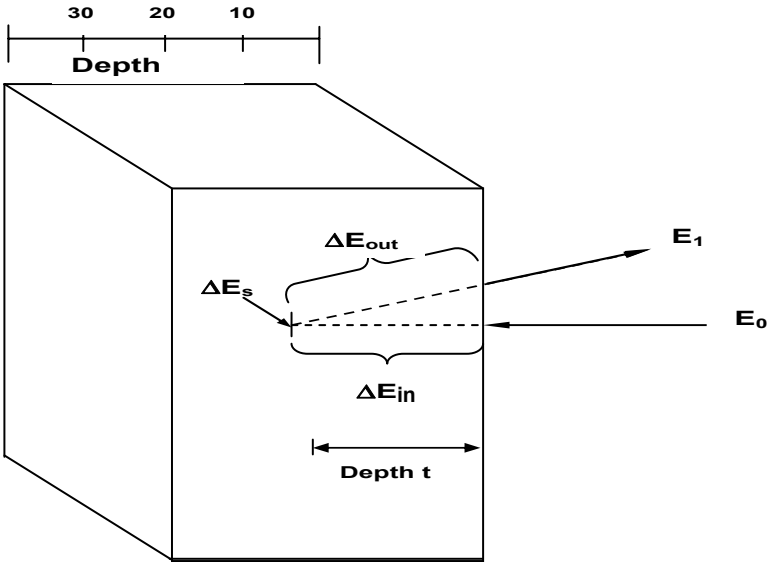

Figure 2.2. Energy loss components for a projectile that scatters from depth t. The particle loses energy ΔE_{in} via inelastic collisions with electrons along the inward path. There is energy loss ΔE_s in the elastic scattering process at depth *t*. There is energy lost to inelastic collisions ΔE_{out} along the outward path.

An example illustrating the influence of depth on analysis is given in Figure 2.3, which shows two thin silver layers on the front and back of a titanium film. The scattering from silver at the surface is clearly separated from Ag at the back layer. The energy width between the Ag signals is closely equal to that of the energy width of the Ti signal. The depth scales are determined from energy loss values.

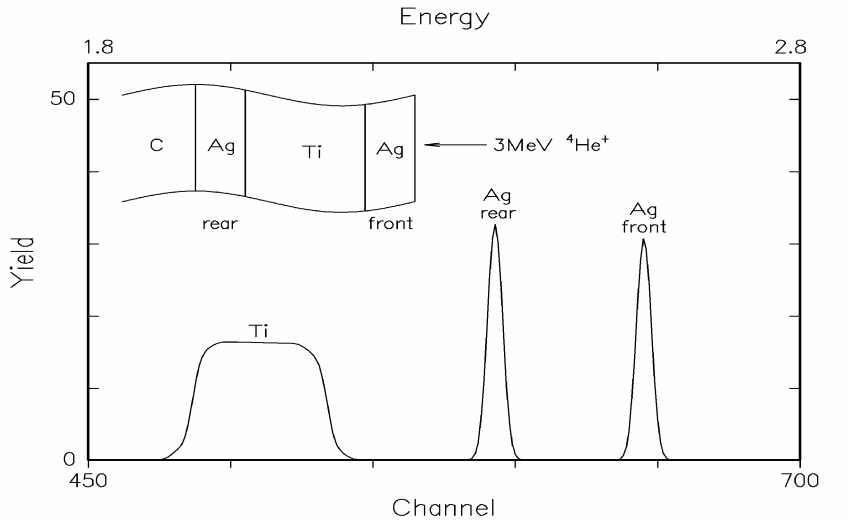

Figure 2.3. Backscattering spectrum of a Ti film (150 nm) with thin layers of Ag (3 nm) on the front and back surfaces of the titanium

2.2.4 Ion Resonances

At energies of a few MeV nuclear reactions and strong deviations from Rutherford scattering can result in a strong increase (resonance) in the scattering cross section (for example at 3.04 MeV for ^{4}He ions incident on ^{16}O). This reaction can be used to increase the sensitivity for the detection of oxygen as well as other light elements such as carbon and nitrogen. In order to evaluate the amount of oxygen in Ag diffusion barriers (*e.g.*, $TiAl_xN_yO_z$) on SiO_2/Si substrate, the oxygen resonance technique using 3.05 MeV $^4He^{+2}$ ion beam was employed (Figure 2.4). The RUMP simulation [7] overlaps the collected spectrum. The enhanced oxygen peak near channel 200 is a direct consequence of O resonance at 3.05 MeV and corresponds to oxygen atoms present in the thin film.

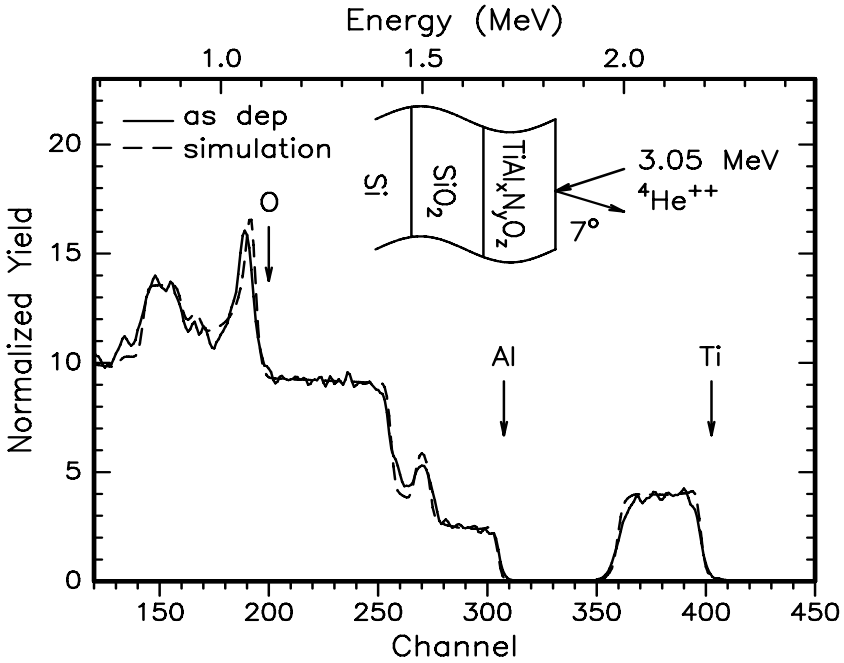

Figure 2.4. RBS spectrum (3.05 MeV He^{+2}, 7° tilt) and simulation of as-deposited $TiAl_xN_yO_z$ thin film on SiO_2/Si substrate

2.3 X-ray Diffractometry

W. L. Bragg derived a description of coherent scattering from an array of periodic scattering sites, *i.e.*, atoms in a crystalline solid. The scalar description of diffraction considers the case of monochromatic radiation impinging on two sheets of atoms in the crystal spaced d_{hkl} between reflecting planes. The wavelength λ of the radiation is smaller than the interatomic spacing d_{hkl} of the specific (*hkl*) planes.

Bragg invoked the Law of Reflectivity (or Reflections) that states that the scattering incident angle and exiting angle must be equal, $\vartheta_{in} = \vartheta_{out}$ under the condition of coherent scattering. The wavelets scattered by the atoms combine to produce constructive interference if the total path difference $2*\Delta P$ for the reflected waves equals integer (n) multiples of λ:

$$n\lambda = 2\Delta P = 2d_{hkl} \sin\vartheta \tag{2.5}$$

Hence, Bragg's Law: $n\lambda = 2d_{hkl} \sin\vartheta$ defines the condition for diffraction. The simplest of all modern X-ray analyses is powder analysis using an X-ray diffractometer. The technique can be used to characterize polycrystalline thin films

as well. The sample under investigation is placed on the sample stage of the diffractometer. The key components of a typical diffractometer include a sample stage, monochromatic radiation source, and radiation electronic solid-state detection system. The scattered X-rays dissipate energy by generation of electron-hole pairs in the detector. The electronic system converts the collected charge into voltage pulses which are directly proportional to the intensity of the diffracted X-ray beam. The typical X-ray spectrum is a plot of intensity verses angle, *e.g.*, 2ϑ. The phase can be indentified by comparing the spectrum to Joint Committee on Powder Diffraction Standards (JCPDS) cards. Figure 2.5 shows an typically XRD spectrum from a 200 nm thick, polycrystalline Ag layer on a single crystalline Si substrate.

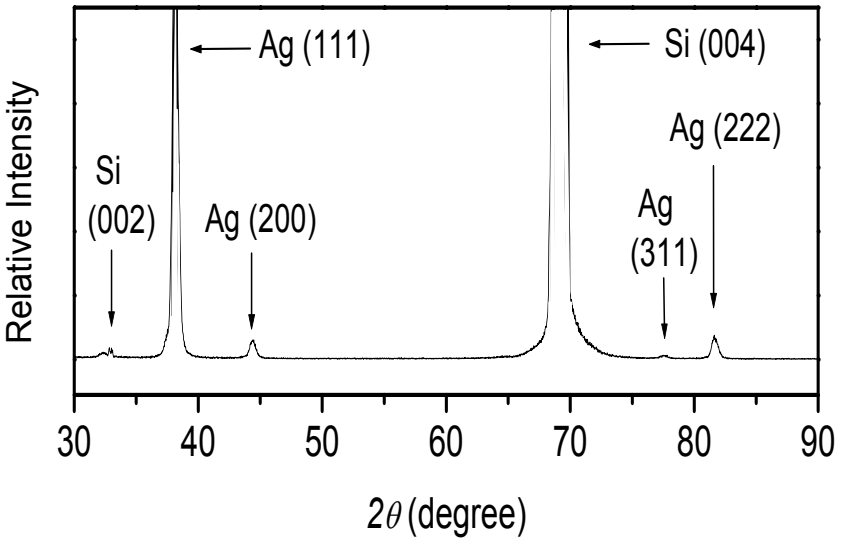

Figure 2.5. XRD spectrum of a 200 nm polycrystalline Ag layer on a single crystalline Si substrate. The indexed peaks correspond to specific reflections. The forbidden Si(002) reflection is due the double difraction of the strong (004) reflection.

2.4 References

[1] W. K. Chu, J. W. Mayer, and M. A. Nicolet, Backscattering Spectrometry, Academic Press, New York, 1978.

[2] J. W. Mayer, E. Rimini, Ion Handbook for Material Analysis, Academic Press, New York, 1977.

[3] B. D. Cullity and S. R. Stock, Elements of X-ray Diffraction, Prentice Hall, NJ, 2001.

[4] T. L. Alford, Feldman, L. C.; J. W. Mayer, Fundamentals of Nanoscale Analysis, Springer, New York, 2007.

[5] S. W. De Coster, B. Brijs, J. Goemans, and W. Vandervost, Nucl. Instr. Meth. B 66**,** 128318(1992).
[6] S. W. Russell, T. E. Levine, A. E. Bair, and T. L. Alford, Nucl. Instr. Meth. B 118**,** 118(1996).
[7] L. R. Doolittle, Nucl. Instr. Meth. B 15, 227(1986).